Influence of interface sink strength on the reduction of radiation-induced defect concentrations and fluxes in materials with large interface area per unit volume

M. J. Demkowicz,[1,*] R. G. Hoagland,[2] B. P. Uberuaga,[2] and A. Misra[3]

[1]*Department of Materials Science and Engineering, Massachusetts Institute of Technology, Cambridge, Massachusetts 02139, USA*

[2]*MST-8: Structure-Property Relations Group, Los Alamos National Laboratory, Los Alamos, New Mexico 87545, USA*

[3]*Center for Integrated Nanotechnologies (CINT), Los Alamos National Laboratory, Los Alamos, New Mexico 87545, USA*

We use a reaction–diffusion model to demonstrate that buried interfaces in polycrystalline composites simultaneously reduce both the concentrations and the fluxes of radiation-induced defects. The steady-state radiation-induced defect concentrations, however, are highly sensitive to the interface sink strength η. Materials containing a large volume fraction of interfaces may therefore be resistant to multiple forms of radiation-induced degradation, such as swelling and hardening, as well as to embrittlement by solute segregation, provided that the interfaces have suitable η values.

I. INTRODUCTION

Radiation-resistant materials have long been recognized as critical to making nuclear energy generation maximally safe, clean, and economical.[1] 'Radiation damage of materials' however, does not refer to a single problem. Rather, it is an umbrella term for a host of degradation modes, such as swelling,[2] hardening,[3,4] and embrittlement.[5] In addition, mitigating one mode may exacerbate another.

For instance, buried interfaces (i.e., interfaces between adjacent components in a composite) are sinks for radiation-induced point defects[6–9] and may reduce swelling and hardening. In alloys, however, they are the cause of radiation-induced segregation (RIS) of solutes,[10,11] which in turn enhances corrosion and embrittlement. Therefore, there may be a tradeoff between decreasing radiation-induced defect concentrations by increasing their flux to interfaces and decreasing defect fluxes to inhibit RIS.

In this paper, we use a reaction–diffusion model to show that maximizing the area per unit volume of buried interfaces simultaneously reduces both concentrations and fluxes of radiation-induced defects. However, the radiation response of materials where the greatest reductions in both are achievable shows extreme sensitivity to the sink strength η of the interfaces. Design of materials for radiation resistance thus requires both a high interface area per unit volume and the control of η.

We base our model on composites of alternating layers of different phases, each of thickness l. Examples include multilayers synthesized using sputter deposition[12] and accumulated roll bonding[13] or lath martensite morphologies in ferritic/martensitic steels.[14] The interfaces between neighboring layers are sinks of varying efficiency for point defects.[9,15] Their area per unit volume equals $1/l$ and so may be controlled by choosing l. Some of these materials have proved remarkably stable under irradiation, exhibiting no intermixing or breakdown in layered morphology after sustaining several displacements per atom (dpa) of damage,[9,16] even at elevated temperatures[17] or when the successive layers are as thin as 2 nm.[18]

Furthermore, multilayer composites are ideal model systems for studying the effect of interfaces on radiation response.

Their periodic morphology may be analyzed in one spatial dimension using a reaction–diffusion model of a single crystalline layer bounded by two interfaces, as shown in Fig. 1. We expect, however, that the qualitative conclusions of our study will hold for materials with more complex morphologies.

II. REACTION–DIFFUSION MODEL

Composite materials may exhibit a variety of responses to radiation, such as phase transformations, microstructure changes, or enhanced susceptibility to aggressive chemical environments.[4] Nevertheless, to isolate the effect of interfaces and their sink strength η on radiation-induced defect concentrations and fluxes, it is convenient to study a simplified model.

We consider only two species of radiation-induced defects: isolated vacancies and self-interstitials. This assumption corresponds well to light ion irradiation, which has been used in many experimental studies on multilayers.[9] Our model accounts for the creation of vacancy–interstitial pairs at a constant and uniform rate, their diffusion, and mutual annihilation.

We begin with a model in which there are no defect sinks besides interfaces. This assumption is experimentally justified in several multilayer composites. For example, transmission electron microscopy and x-ray diffraction investigations have not found appreciable quantities of dislocations or precipitates in as-synthesized and even severely plastically deformed Cu-Nb composites with sufficiently thin layers.[19,20] Absence of dislocation substructures is attributed to efficient dislocation trapping at interfaces,[21] whereas lack of precipitates is due to the well-controlled synthesis procedure, which does not introduce impurities, as well as absence of intermixing.[12,13] We show in Sec. III that our conclusions are not sensitive to this assumption by introducing hypothetical sinks with a bias for absorbing interstitials into our model.

Clustering of vacancies and interstitials has also been neglected. This assumption holds for sufficiently high temperatures, low collision energies, low irradiation rates, or low defect concentrations.[4] Should defect clusters form, however, they would also act as sinks for point defects and could diffuse independently.
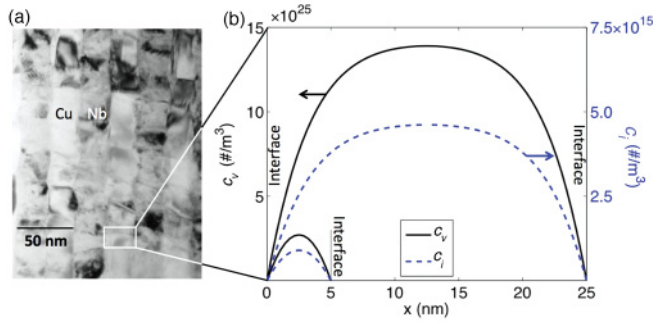
FIG. 1. (Color online) (a) The multilayer morphology motivates (b) the one-dimensional reaction–diffusion model of a crystalline layer bounded by two interfaces. c_v and c_i in this plot were obtained at $T = 300$K and $K_0 = 10^{25}$m^{3}s using the parameters in Table I for $l = 25$ and 5 nm. The solution for 1 = 5 nm is shown in the bottom left corner in (b). Note the reduction of average defect concentrations and concentration gradients near interfaces for $l = 5$ nm compared to $l = 25$ nm.

Under these assumptions, the concentrations c_v and c_i of vacancies and interstitials, respectively, are described by the coupled reaction–diffusion equations

$$\frac{\partial c_v}{\partial t} = D_v \frac{\partial^2 c_v}{\partial x^2} + K_0 - K_{iv} c_v c_i$$
$$\frac{\partial c_i}{\partial t} = D_i \frac{\partial^2 c_i}{\partial x^2} + K_0 - K_{iv} c_v c_i, \tag{1}$$

where K_0 is the vacancy–interstitial pair creation rate, K_{iv} is their recombination rate coefficient, and D_v and D_i are vacancy and interstitial diffusivities, respectively.

We investigate defect concentrations once a time-invariant steady state has been reached. The only time scales in our model are (1) the time for defect recombination and creation rates to balance in the absence of diffusion and (2) the diffusion times over distance l. The former is proportional to $(K_{iv}K_0)^{-1/2}$ and is on the order of microseconds for room temperature He implantation in metals.[4,9,22] The latter is proportional l^2/D and equals $\sim$12.5 ns for interstitials and $\sim$20 s for vacancies at room temperature in a 10-nm-thick Cu layer. The steady-state assumption is therefore justified in implantation studies of metal multilayers, which typically last several hours. It might not hold at cryogenic temperatures or in ceramics, where defect diffusivities are much lower than in metals.

Setting the time derivatives in Eq. (1) to zero, introducing the changes in variables

$$x = \frac{l}{2} y$$

$$c_v = \sqrt{\frac{K_0 D_i}{K_{iv} D_v}} (m + n) \tag{2}$$

$$c_i = \sqrt{\frac{K_0 D_v}{K_{iv} D_i}} (n - m)$$

(m and n are scaled concentration variables expressible in terms of c_v and c_i using the definitions in Eq. (2)), and

assuming concentration-independent diffusivities, the governing equations become

$$\frac{\partial^2 m}{\partial y^2} = 0 \tag{3a}$$

and

$$(1 + m^2) - n^2 + s \frac{\partial^2 n}{\partial y^2} = 0 \tag{3b}$$

where $s = \sqrt{\frac{16 D_v D_i}{l^4 K_0 K_{iv}}}$. Integrating Eq. (3a) and using Eq. (2) gives

$$\frac{\partial m}{\partial y} = \text{const.} \Rightarrow D_v \frac{\partial c_v}{\partial x} - D_i \frac{\partial c_i}{\partial x} = \text{const.}, \tag{4}$$

i.e., the difference between vacancy and interstitial fluxes is constant throughout the layer.

Because our model geometry is symmetrical about the layer midpoint, we apply a no-flux boundary condition at $x = l/2$: $\frac{\partial c_v}{\partial x}|_{l/2} = \frac{\partial c_i}{\partial x}|_{l/2} = 0$. Together with Eq. (4), this says that steady-state vacancy and interstitial fluxes are equal throughout the layer. In particular, point defects arrive at interfaces at equal rates, allowing their continuous trapping and recombination without a buildup of either.

Integrating $\frac{\partial m}{\partial y} = 0$ and using Eq. (2), we obtain $m = \sqrt{\frac{K_{iv}}{4 K_0 D_v D_i}} (D_v c_v - D_i c_i) = \text{const.}$ Thus, in the absence of distributed sinks, steady-state vacancy and interstitial concentrations are related through the constant m, regardless of location within the sample or boundary conditions applied at the interfaces. To assign a specific value to m, we assume that c_v and c_i have equilibrated with distant free surfaces, where they take on thermal equilibrium values, $c_v = c_v^e, c_i = c_i^e$. Elsewhere, c_v and c_i may have other values even though these are related through the constant value of m, as set at the free surfaces. The free surfaces are not explicitly modeled but must be present in any real material. A different value of m would simply alter the first term on the left-hand side of Eq. (3b).

If the interfaces are perfect sinks, we have at $x = 0$ (directly adjacent to an interface)

$$c_v|_0 = c_v^e, \quad c_i|_0 = c_i^e. \tag{5}$$

For an imperfect sink interface, we define the sink strength η as the ratio of defect flux into that interface ($J_{\text{imperfect}}$) to the defect flux into a perfect sink interface (J_{perfect})[23]:

$$\eta = \frac{J_{\text{imperfect}}}{J_{\text{perfect}}}. \tag{6}$$

Because the fluxes of vacancies and interstitials throughout the layer are equal, different values of η are not needed for these two defect types. To study the influence of η, we first solve our model for a perfect sink interface using the boundary conditions in Eq. (5), find the defect flux J_{perfect}, and then solve again under the new boundary conditions: $-D_v \frac{\partial c_v}{\partial x}|_0 = -D_i \frac{\partial c_i}{\partial x}|_0 = \eta J_{\text{perfect}}$.

With $m = \text{const.}$, Eq. (3b) may be multiplied by $\frac{\partial n}{\partial y}$ and integrated with respect to y, yielding

$$(1 + m^2) n - \frac{1}{3} n^3 + \frac{1}{2} s \left(\frac{\partial n}{\partial y} \right)^2 = C, \tag{7}$$

TABLE I. Parameters for Cu used in the numerical solution of the reaction–diffusion model. The diffusivity of defect a is computed as $D_a = a_{Cu}^2 \nu_a e^{-\Delta E_a^m / k_B T}$.

Quantity	Value
Cubic lattice parameter, a_{Cu}	3.615 Å
Vacancy formation energy, ΔE_v^f	1.26 eV
Interstitial formation energy, ΔE_i^f	3.24 eV
Vacancy migration energy, ΔE_v^m	0.69 eV
Interstitial migration energy, ΔE_i^m	0.084 eV
Vacancy migration attempt frequency, ν_v	3.36×10^{13}/s
Interstitial migration attempt frequency, ν_i	6.67×10^{12}/s

where C is a constant of integration that depends on l and boundary conditions. The solution to this equation is the Weierstrass P-function.[24] We are not aware of any convenient analytical method of computing the value of C for a given l and boundary conditions, so instead we investigate the solutions to Eq. (3b) numerically using material parameters appropriate to Cu. These were obtained from the Voter Cu embedded atom method (EAM) potential[25] and are given in Table I.

The defect recombination rate coefficient was computed as $K_{iv} = N_r a_{Cu}(D_v + D_i)$, where N_r is the number of sites surrounding a vacancy where introduction of an interstitial leads to spontaneous recombination (following Ref. 4, we take $N_r = 12$) and a_{Cu} is the cubic lattice parameter of Cu. Using the Stopping and Range of Ions in Matter (SRIM) program,[26] we find that $K_0 \approx 10^{25}$/m^{3}s for typical He ion implantation experiments[9] and $K_0 \approx 10^{20}$/m^{3}s is more appropriate for nuclear reactor conditions.[1] The boundary value problem that describes our model was solved using the collocation method implemented in MATLAB.

III. RADIATION-INDUCED DEFECT CONCENTRATIONS AND FLUXES

Figure 1(b) shows a typical solution for c_v and c_i with temperature $T = 300$K for $l = 25$ and 5 nm. c_v and c_i have the same shape but differ by a large multiplicative factor arising from the much higher diffusivity of interstitials compared to vacancies. For $l = 25$ nm, within ∼5 nm of each interface, vacancy and interstitial concentrations are reduced compared to the layer midpoint $x = l/2$. For $l = 5$ nm, these zones overlap, decreasing both the average defect concentrations in the layer and the concentration gradients near the interface. For sufficiently large l, the effect of these zones is negligible.

We investigated defect concentrations and fluxes for l in the range 1–100 nm and temperatures T of 300–700 K. In this parameter range, interfaces have a significant effect on average defect concentrations. We define a defect concentration measure $P_a = \bar{c}_a / c_a^\infty$ ($a = v, i$), where $\bar{c}_a = \frac{2}{l}\int_0^{l/2} c_a(x) dx$ is the average concentration in a crystalline layer of thickness l and c_a^∞ is the average concentration in an infinitely thick layer. Similarly, for fluxes we define $Q = J_{x=0}/J_{x=0}^\infty$, where $J_{x=0}$ is the flux of defects into an interface for a layer of given l and $J_{x=0}^\infty$ is the flux in an infinitely thick layer.

Figures 2(a)–2(c) and 2(e)–2(g) show contour plots of $\log_{10}(P_v)$, $\log_{10}(P_i)$, and $\log_{10}(Q)$ as functions of l and T for two different K_0 values. For $K_0 = 10^{20}$/m^{3}s, 350 K $< T <$ 500 K, and $l < 10$ nm, the average radiation-induced interstitial concentration is reduced by as much as seven orders of magnitude and the defect flux to the interface is simultaneously reduced by three orders of magnitude. In this range of T and l, the vacancy concentration is also reduced by as many as six orders of magnitude. For sufficiently high T, however, P_v approaches unity and becomes l-independent
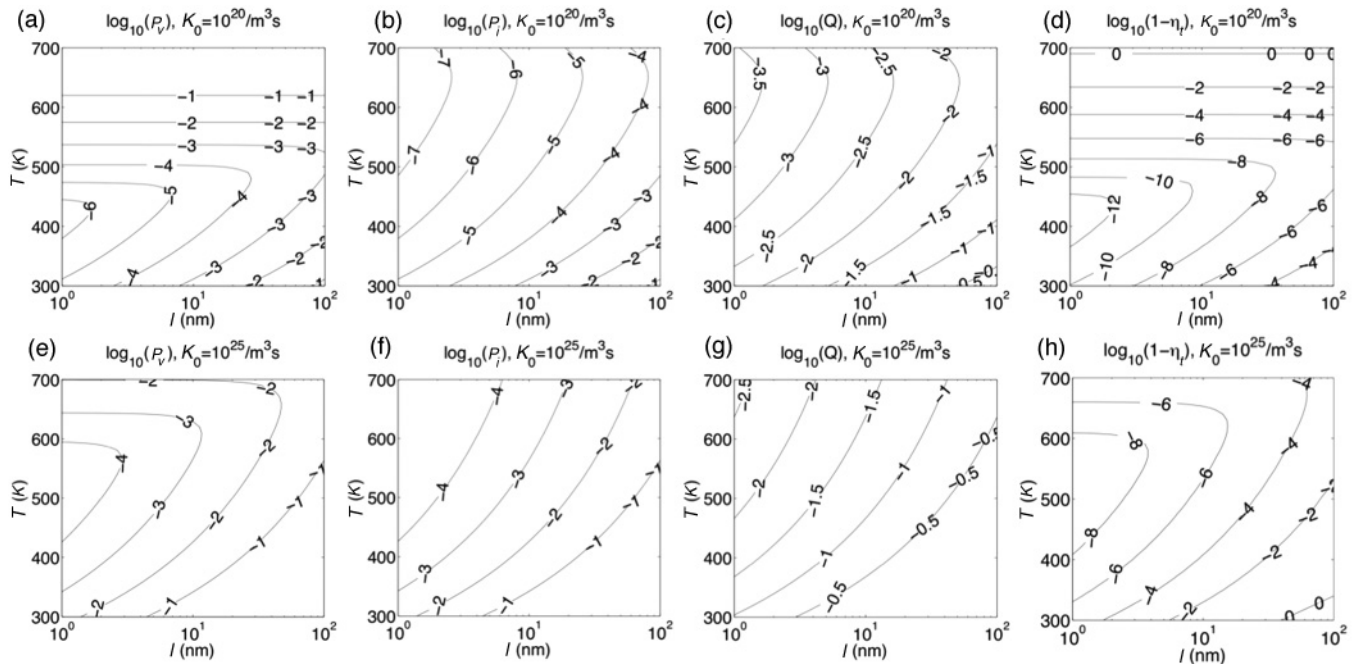

FIG. 2. The dependence on l and T of (a) and (e) $\log_{10}(P_v)$, (b) and (f) $\log_{10}(P_i)$, (c) and (g) $\log_{10}(Q)$, and (d) and (h) $\log_{10}(1 - \eta_t)$.
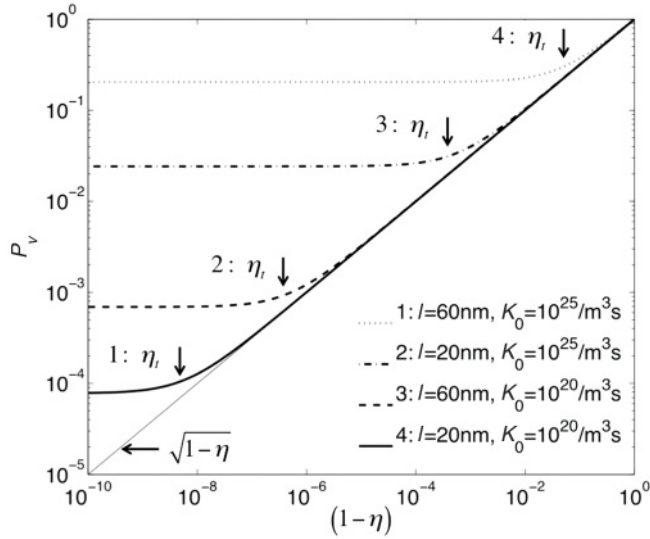
FIG. 3. For given irradiation conditions, there is a transitional sink strength η_t above which P_v is insensitive to η and below which P_v varies as $\sqrt{1-\eta}$. All plots in this figure are for $T = 450$K.

as the thermal equilibrium vacancy concentration reaches and eventually exceeds the radiation-induced one. Similar trends may be seen for $K_0 = 10^{25}/m^3s$. Evidently, increasing interface area per unit volume simultaneously minimizes both defect concentrations and fluxes in a technologically important range of temperatures[1] for both ion implantation and nuclear reactor conditions.

Figure 3 shows the dependence of P_v on $(1 - \eta)$ for several example sets of irradiation conditions (all at $T = 450$ K but differing in l and K_0 as stated in the figure legend). In each case, there is a transitional sink strength value η_t above which P_v is η-independent and below which P_v varies as $\sqrt{1-\eta}$. The dependence of Q on η follows directly from Eq. (6).

Defining η_t as the value of η at which P_v exceeds the perfect sink case by 20%, we computed η_t for a variety of irradiation conditions and plot $\log_{10}(1 - \eta_t)$ in Fig. 2(d) and 2(h). The lowest values of $(1 - \eta_t)$ occur in the range of T and l, where the greatest reductions in vacancy concentration and flux are achievable. Because $P_v \sim \sqrt{1 - \eta}$ when $\eta < \eta_t$, for η_t close to unity, even modest decreases in η may cause P_v to increase by orders of magnitude, dramatically reducing the effectiveness of interfaces in removing radiation-induced point defects. Thus, synthesis of materials that simultaneously minimize both the concentration and the flux of radiation-induced defects requires not only a large interface area per unit volume but also the control of interface sink strength η.

We repeated our calculations for systems containing biased sinks in concentrations equivalent to dislocation densities of $10^{12}–10^{14}/m^2$ and found that the qualitative behavior is unaffected: under all conditions, there exists a transition sink strength η_t, and the value of $(1 - \eta_t)$ is lowest for T and l, where defect concentrations and fluxes may be most markedly reduced by increasing interface area. Below η_t, P_v varies as $\sqrt{1 - \eta}$ for low sink concentrations. For high sink concentrations, it varies as $(1 - \eta)$ for η just below η_t but resumes the $\sqrt{1 - \eta}$ trend with decreasing η. When

biased sinks are included in the reaction–diffusion model, the difference between vacancy and interstitial fluxes is no longer constant and vacancy and interstitial concentrations are not related through the constant m. Our conclusions therefore do not depend on such special features characteristic of Eq. (1).

IV. DISCUSSION AND CONCLUSIONS

Early analytical studies of the effect of buried interfaces on radiation-induced defect concentrations only considered one defect type—usually vacancies—and modeled recombination using an effective sink term with the coefficient K_{sv}.[27] This approach is simpler than ours; instead of the nonlinear, coupled system in Eq. (1), it gives rise to just one linear differential equation:

$$\frac{\partial c_v}{\partial t} = D_v \frac{\partial^2 c_v}{\partial x^2} + K_0 - K_{sv}c_v. \tag{8}$$

Solving this equation under steady-state conditions for interfaces with sink strength η, the following analytical expression for the vacancy concentration measure P_v is obtained:

$$P_v = 1 - \eta\left(1 - \frac{K_{sv}c_v^e}{K_0}\right)r. \tag{9}$$

Here, $r = (\frac{2}{l}\sqrt{\frac{D}{K_{sv}}})tanh(\frac{l}{2}\sqrt{\frac{K_{sv}}{D}})$ is a factor that does not depend on η. Thus, when recombination is neglected, P_v varies linearly with η and the model predicts neither the transitional sink strength η_t nor the square root dependence of P_v on $(1 - \eta)$. Both of these features arise from the explicit inclusion of bulk recombination in our model. Several other authors have studied the reaction–diffusion model in Eq. (1),[22,28] and some have even assessed rigorously the impact of treating recombination as an effective sink.[27,29] Nevertheless, the effect of interface sink strength η was not investigated in these previous studies, so the sensitivity of radiation-induced defect concentrations to η was not noticed.

The difference between the single- and the two-defect cases just described suggests that studies of interface sink strength carried out using quenched-in vacancy concentrations may not provide interface behavior representative of irradiation.[30] However, both the single- and the two-defect approaches show that the flux and the concentration of defects become smaller with decreasing l.

We have shown that interfaces, if present in high enough densities, may simultaneously reduce average radiation-induced defect concentrations and defect fluxes to the interfaces. This implies that interfaces may be used to control multiple radiation-induced failure modes, including void swelling, hardening, and RIS, and thus offer one route to designing materials that withstand several forms of radiation damage.

However, radiation-induced defect concentrations increase rapidly as η drops below η_t. Thus, a material with a high density of interfaces whose sink strength is below the transitional value η_t may be far less radiation resistant than would be expected if all interfaces were perfect sinks. Design of radiation-resistant composites therefore requires not only maximizing the interface area per unit volume but also controlling η.

The sink strength η of an interface depends on its structure and the detailed mechanisms by which it interacts with point defects. For example, Balluffi and Granato derived an expression for η of tilt grain boundaries under diffusion-controlled conditions, assuming that point defects are trapped at jogs on edge misfit dislocations in these boundaries. They obtained $\eta = 1/(1 + \ln(cd_s)d_s/d_d)$, where d_s is the average distance between point defect trapping sites within the boundary, d_d is the characteristic defect diffusion distance to the boundary, and c is a constant.[31] Therefore, η is close to unity for small d_s (which may be characteristic of many grain boundaries[32]) and decreases rapidly with increasing d_s.

Relations between the detailed structure of general, heterophase interfaces and their sink strengths under irradiation are currently not available. Should they be developed, it may become possible to control η by tailoring the heterophase interface character distribution in composite materials, in analogy to grain boundary engineering in homophase polycrystals.[33,34]

*demkowicz@mit.edu

[1] Y. Guerin, G. S. Was, and S. J. Zinkle, MRS Bull. **34**, 10 (2009).

[2] L. K. Mansur, Nucl. Tech. **40**, 5 (1978).

[3] B. N. Singh, A. J. E. Foreman, and H. Trinkaus, J. Nucl. Mater. **249**, 103 (1997).

[4] G. S. Was, *Fundamentals of Radiation Materials Science: Metals and Alloys* (Springer, Berlin, 2007).

[5] G. R. Odette and G. E. Lucas, JOM **53**, 18 (2001).

[6] B. N. Singh, Philos. Mag. **29**, 25 (1974).

[7] Y. Chimi, A. Iwase, N. Ishikawa, A. Kobiyama, T. Inami, and S. Okuda, J. Nucl. Mater. **297**, 355 (2001).

[8] N. Nita, R. Schaeublin, M. Victoria, and R. Z. Valiev, Philos. Mag. **85**, 723 (2005).

[9] A. Misra, M. J. Demkowicz, X. Zhang, and R. G. Hoagland, JOM **59**, 62 (2007).

[10] P. R. Okamoto and L. E. Rehn, J. Nucl. Mater. **83**, 2 (1979).

[11] H. Wiedersich, P. R. Okamoto, and N. Q. Lam, J. Nucl. Mater. **83**, 98 (1979).

[12] T. E. Mitchell, Y. C. Lu, A. J. Griffin, M. Nastasi, and H. Kung, J. Am. Ceram. Soc. **80**, 1673 (1997).

[13] S. C. V. Lim and A. D. Rollett, Mater. Sci. Eng. A **520**, 189 (2009).

[14] R. L. Klueh, Int. Mater. Rev. **50**, 287 (2005).

[15] M. J. Demkowicz, R. G. Hoagland, and J. P. Hirth, Phys. Rev. Lett. **100**, 136102 (2008).

[16] T. Hochbauer, A. Misra, K. Hattar, and R. G. Hoagland, J. Appl. Phys. **98**, 123516 (2005).

[17] K. Hattar, M. J. Demkowicz, A. Misra, I. M. Robertson, and R. G. Hoagland, Scr. Mater. **58**, 541 (2008).

[18] X. Zhang, N. Li, O. Anderoglu, H. Wang, J. G. Swadener, T. Hochbauer, A. Misra, and R. G. Hoagland, Nucl. Inst. Meth. B **261**, 1129 (2007).

[19] A. Misra and R. G. Hoagland, J. Mater. Sci. **42**, 1765 (2007).

[20] K. Nyilas, A. Misra, and T. Ungar, Acta Mater. **54**, 751 (2006).

[21] J. Wang, R. G. Hoagland, J. P. Hirth, and A. Misra, Acta Mater. **56**, 5685 (2008).

[22] R. Sizmann, J. Nucl. Mater. **69-7**, 386 (1978).

[23] A. P. Sutton and R. W. Balluffi, *Interfaces in Crystalline Materials* (Oxford University Press, Oxford, 1995).

[24] V. V. Prasolov and I. U. P. Solovyev, *Elliptic Functions and Elliptic Integrals* (American Mathematical Society, Providence, RI, 1997).

[25] A. F. Voter, LANL Unclassified Technical Report # LA-UR 93-3901 (1993).

[26] J. F. Ziegler, J. P. Biersack, and U. Littmark, *The Stopping and Range of Ions in Solids* (Pergamon, New York, 1985).

[27] R. Bullough, M. R. Hayns, and M. H. Wood, J. Nucl. Mater. **90**, 44 (1979).

[28] N. Q. Lam, S. J. Rothman, and R. Sizmann, Radiat. Eff. Defects Solid. **23**, 53 (1974).

[29] A. D. Brailsford, J. R. Matthews, and R. Bullough, J. Nucl. Mater. **79**, 1 (1979).

[30] R. W. Siegel, S. M. Chang, and R. W. Balluffi, Acta Metall. **28**, 249 (1980).

[31] R. W. Balluffi and A. V. Granato, in *Dislocations in Solids*, edited by F. R. N. Nabarro (North-Holland, New York, 1979), pp. 1–133.

[32] C. A. Schuh, M. Kumar, and W. E. King, Z. Metallkd. **94**, 323 (2003).

[33] L. Tan, K. Sridharan, T. R. Allen, R. K. Nanstad, and D. A. McClintock, J. Nucl. Mater. **374**, 270 (2008).

[34] T. Watanabe and S. Tsurekawa, Mater. Sci. Eng. A **387**, 447 (2004).